

# Ultrafast Excited State Dynamics and Fluorescence from Vitamin B<sub>12</sub> and Organometallic [Co]–C≡C–R Cobalamins

Elvin V. Salerno, Nicholas A. Miller, Arkaprabha Konar, Yan Li, Christoph Kieninger, Bernhard Kräutler, and Roseanne J. Sension\*

Cite This: *J. Phys. Chem. B* 2020, 124, 6651–6656

Read Online

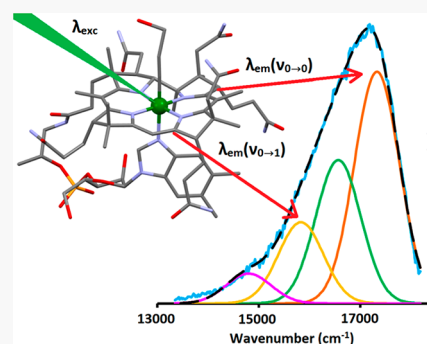
ACCESS |

Metrics & More

Article Recommendations

Supporting Information

**ABSTRACT:** Cobalamins are cobalt-centered cyclic tetrapyrrole ring-based molecules that provide cofactors for exceptional biological processes and possess unique and synthetically tunable photochemistry. Typical cobalamins are characterized by a visible absorption spectrum consisting of peaks labeled  $\alpha$ ,  $\beta$ , and  $\text{sh}$ . The physical basis of these peaks as having electronic origin or as a vibronic progression is ambiguous despite much investigation. Here, for the first time, cobalamin fluorescence is identified in several derivatives. The fluorescence lifetime is ca. 100–200 fs with quantum yields on the order of  $10^{-6}$ – $10^{-5}$  because of rapid population of “dark” excited states. The results are compared with the fluorescent analogue with zinc replacing the cobalt in the corrin ring. Analysis of the breadth of the emission spectrum provides evidence that a vibrational progression in a single excited electronic state makes the dominant contribution to the visible absorption band.



## INTRODUCTION

Light is an abundant and versatile energy source, essential as a basis for all forms of higher life,<sup>1,2</sup> and provides a tool for the manipulation and control of molecular scale devices.<sup>3,4</sup> Metal-coordinating cyclic tetrapyrroles including chlorins, porphyrins, and corrins (in vitamin B<sub>12</sub> derivatives) are employed for a wide range of light-activated applications, from light harvesting and energy conversion to gene regulation and delivery of therapeutic agents.<sup>3–6</sup> Excitation in the visible or near-UV region of the spectrum takes advantage of intense  $\pi\pi^*$  transitions carrying the oscillator strength for absorption.<sup>2,7</sup> Photochemistry of (open shell) transition metal complexes, on the other hand, is controlled by metal-to-ligand charge transfer states, ligand-to-metal charge transfer states, and/or metal-centered states.<sup>8</sup> The transitions between these states have been the subject of many different experimental and theoretical studies.<sup>8–10</sup>

Cobalamins (Cbls, Figure 1) comprise a unique class of cyclic tetrapyrroles with a cobalt ion bonded to a corrin ring, a lower dimethylbenzimidazole ligand (DMB) covalently tethered to the corrin ring, and a variable upper axial ligand.<sup>11–13</sup> The lower axial DMB ligand can be replaced with histidine in some enzymes<sup>14</sup> or by water in a protonated base-off configuration at low pH<sup>15</sup> and is decoordinated without replacement in some proteins.<sup>16–18</sup> B<sub>12</sub>-dependent enzymes exploit the distinct reactive pathways of two organometallic Cbls: 5'-deoxyadenosylcobalamin (coenzyme B<sub>12</sub> or AdoCbl) and methylcobalamin (MeCbl).<sup>19–21</sup> These Cbls are also light sensitive and undergo photoinduced homolysis of their Co–C bond.<sup>8–10</sup> The unique Co–C bond of organometallic Cbls also

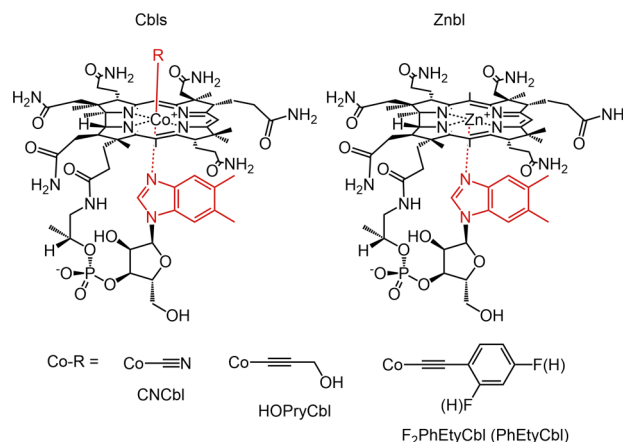


**Figure 1.** Schematic structure of cobalamins (Cbls), with the specific R groups investigated here, and of the zinc analogue zinccobalamin (Znbl).

provides space for chemical manipulation of both their thermal and photochemical reactivity.<sup>13,22–24</sup> Strong Co–C bonds and their photochemical stability are exploited in a range of alkynyl cobalamins<sup>23,25,26</sup> designed as potential antivitamin B<sub>12</sub>.<sup>27</sup>

Received: May 30, 2020

Revised: June 30, 2020

Published: July 21, 2020



The influence of axial ligation on cobalamin photochemistry has been the subject of many spectroscopic and theoretical investigations.<sup>8–10,28,29</sup> The vertical electronic transitions to excited states, the nature of the potential energy surfaces of cobalt corrins, and the photochemical pathways depend on the bonding to the axial ligands. Despite extensive study, significant uncertainty remains regarding the nature of the electronic excited state or states responsible for the strong visible absorption band. The  $\alpha$ - and  $\beta$ -bands in the visible absorption spectrum of so-called “typical” cobalamins (Figure 2) along with the shoulder to slightly higher energy are

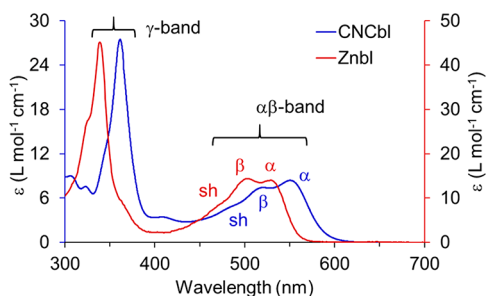


**Figure 2.** Comparison of the absorption spectrum of a typical cobalamin, cyanocobalamin (CNCbl), and zinccobalamin (Znbl). The pertinent band labels are also indicated.

variously assigned to distinct electronic transitions<sup>30–32</sup> or to a vibrational progression dominated by a single electronic transition.<sup>29,33,34</sup> The structure is less pronounced in the  $\alpha\beta$ -band of so-called “atypical” cobalamins, including the biologically active coenzymes AdoCbl and MeCbl (see Figure S1). The absorption spectrum of the zinc analogue zinccobalamin (Znbl),<sup>35</sup> also plotted in Figure 2, is similar to the typical cobalamins, although blue-shifted by ca. 24 nm (800  $\text{cm}^{-1}$ ). The similarity between Znbl and typical cobalamins agrees with the hypothesis that the spectrum is characteristic of  $\pi\pi^*$  transitions of the equatorial corrin. This hypothesis is further supported by comparison of spectra of the metal free hydrogenobyrinic acid (Hby) and zinc-substituted zincobyrinic acid (Znby).<sup>35,36</sup>

In a recent study, triply resonant sum frequency (TRSF) spectroscopy was used to address the question of electronic and vibrational contributions to the absorption spectrum of cyanocobalamin (CNCbl).<sup>33</sup> While this and similar approaches have great potential, the result to date was unable to determine the nature of the absorption bands unambiguously. The conclusion, in favor of a vibrational assignment, considered prior Raman excitation profiles along with the fact that TRSF measurements did not rule out a vibrational assignment, rather than strong positive evidence for a vibrational assignment.

Fluorescence provides another means to distinguish electronic transitions from vibrational sidebands. Fluorescence from the  $\pi\pi^*$  state of the corrin ring has been reported for metal-free corrins.<sup>36–38</sup> The fluorescence spectra of metal-free corrins<sup>36,38</sup> and Zn corrins<sup>35</sup> exhibit varied vibrational structure, providing the strongest evidence to date for a vibrational assignment of the  $\alpha\beta$ -band absorption of “typical” cobalamins.<sup>34,39</sup> The data on the metal free corrins are complicated, however, as their strong emission in the visible features considerable temperature dependence.<sup>36,38</sup> The zinc corrins also exhibit strong fluorescence spectra with a clear vibrational progression,<sup>35</sup> although the rapid decrease in

intensity at longer wavelengths suggests that the entire width of the  $\alpha\beta$ -band in the absorption spectrum cannot be attributed to a vibrational progression in a single electronic state (see below).

Cobalamins are generally considered nonfluorescent. Motion along the reactive surface or internal conversion from the  $\pi\pi^*$  state proceeds rapidly, preventing the observation of emission under most conditions.<sup>8,40,41</sup> In fact, an ultrafast X-ray study of cyanocobalamin (CNCbl) suggests ultrafast motion out of the initial Franck–Condon region from a “bright” corrin-centered  $\pi\pi^*$  electronic configuration to a dark ligand field  $\pi\sigma^*(3d_z^2)$  configuration occurs within ca. 50 fs, followed by elongation of the axial bonds.<sup>42,43</sup> Relaxation into the excited state minimum is complete within a few hundred femtoseconds. However, rapid motion out of the Franck–Condon region only limits the quantum yield of emission; emission can still occur at early times. Very recently, we reported the presence of a short-lived ( $\leq 200$  fs) stimulated emission signal following excitation of AdoCbl at 575 nm on the red edge of the absorption spectrum.<sup>44</sup> Comparison with the transient XANES spectrum of AdoCbl again provided evidence for correlation of the disappearance of the stimulated emission with elongation of one or both axial bonds. The initial structural changes involve ring expansion during which emission is observed; these are followed conversion to a “dark” electronic configuration and axial expansion ca. 200 fs later. However, the overlap of excited state absorption with stimulated emission prevents analysis of the fluorescence spectrum for AdoCbl from these data.<sup>44</sup> The high photolysis yield of AdoCbl complicates attempts to measure the fluorescence spectrum by using traditional methods.

Here we report broadband transient absorption and steady state fluorescence measurements for three photostable cobalamins, CNCbl, 3-hydroxypropynylcobalamin (HO-PryCbl),<sup>25</sup> and 2[4,6-difluorophenyl]ethynylcobalamin (F<sub>2</sub>PhEtyCbl).<sup>26</sup> The results are compared with steady state fluorescence measurements on the zinc corrin Znbl.<sup>35</sup> The measurements reported here demonstrate that the breadth of the  $\alpha\beta$ -band absorption spectrum of typical cobalamins is dominated by a single electronic transition but must also contain contributions from unique electronic transitions at slightly shorter wavelengths.

## EXPERIMENTAL METHODS

Transient absorption measurements were performed by using two Ti:sapphire laser systems producing 808–810 nm pulses at a 1 kHz repetition rate with duration  $< 100$  fs. The ca. 405 nm excitation pulse was generated via 810 nm second harmonic generation in a thin  $\beta$ -barium borate crystal. The 550 nm excitation pulse was produced via a NOPA (home-built or commercial TOPAS White, Light Conversion) which was attenuated to 500 nJ to ensure linear absorbance. Broadband continua were generated by focusing 404 or 808 nm pulses (ca. 500 nJ) into a 5 mm CaF<sub>2</sub> plate. The continuum produced using 404 nm excitation spans  $\sim 270$ –625 nm and was attenuated by a combination of nickel(II) sulfate, cobalt(II) sulfate, and neutral density filter. The continuum produced by using 808 nm excitation spans  $\sim 325$ –800 nm and was attenuated by a KG5 filter (Schott) and neutral density filter. The 15 nJ continuum was focused to a spot size of 70  $\mu\text{m}$  at the sample, while the excitation spot size was 150  $\mu\text{m}$ . The continuum was detected by a Horiba Job Yvon spectrometer (iHR320) coupled to a CCD (Pixis, Princeton Instruments) or

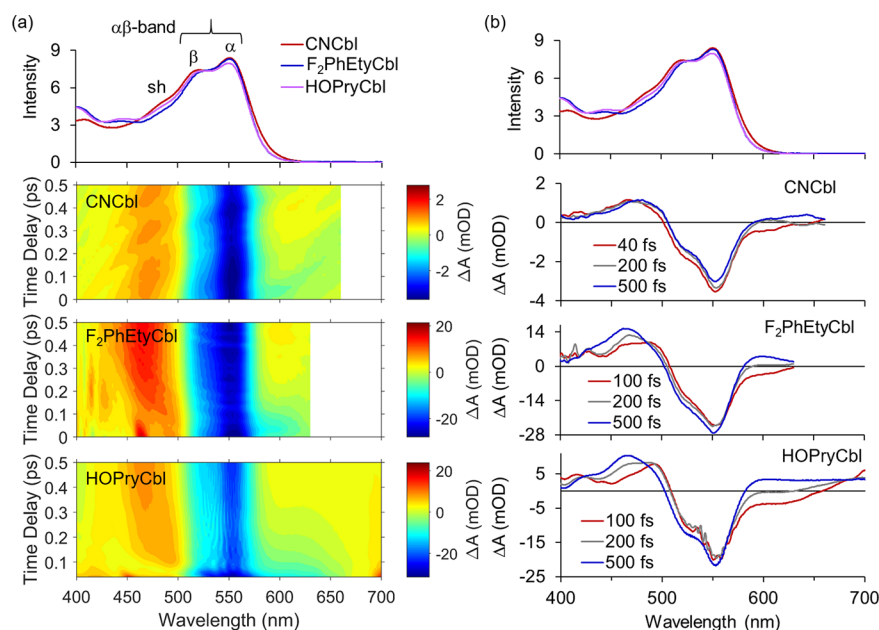


**Figure 3.** (a) Top: visible absorption spectra of CNCbl, F<sub>2</sub>PhEtyCbl, and HOPryCbl in water. The intensity scale represents the extinction coefficient of CNCbl/1000. The other two compounds have been scaled to approximately the same intensity in the visible band. Bottom: surface plots of the transient absorption signal observed over the first 500 fs following excitation of each compound at 550 nm. The stimulated emission is indicated by the transient negative signal ca. 600 nm. (b) Transient difference spectra of CNCbl, F<sub>2</sub>PhEtyCbl, and HOPryCbl averaged around the indicated time delays. There is a clear stimulated emission signal to the red of the ground state bleach between 590 and 650 nm at the earliest times. The steady state spectrum is repeated in the top panel for comparison.

an Avantes spectrometer. The excitation-detection time delays were set by retroreflector and translation stage. The excitation pulses were modulated at 500 Hz by an optical chopper to measure the absorbance difference. Most samples were measured at a concentration of 1 mg/mL in a 1 mm path length cuvette. Cyanocobalamin measurements used a 300  $\mu$ m wire guided flow to eliminate contributions from the cell windows.

Integrated fluorescence measurements on HOPryCbl, F<sub>2</sub>PhEtyCbl, and CNCbl were performed via a Horiba Quanta Master instrument equipped with a xenon arc lamp and photomultiplier tube detector as excitation scans and emission scans. Samples were prepared at concentrations ranging from 5 to 40  $\mu$ M in a 1 cm quartz cuvette. Slit widths were set to 5 nm for both detection and excitation slits, and the integration time was 1 s. An automated photodiode correction was employed.

## RESULTS

The transient absorption spectra for all three Cbls obtained with 550 nm excitation over the first 500 fs are summarized in Figure 3. Line-outs averaged around key time delays are presented in Figure 3b. These transient spectra demonstrate clear evidence for stimulated emission from the initial excited state, evidenced by negative signals at wavelengths between 590 and 650 nm. The stimulated emission contribution has vanished within  $\sim$ 500 fs, leaving only contributions from excited state absorption and the bleaching of the ground state absorption. Thus, evolution out of the Franck–Condon region is complete within a few hundred femtoseconds. If the data are fit to a model consisting of a sum of exponentials, the fluorescence lifetime is  $\sim$ 200 fs for both HOPryCbl and F<sub>2</sub>PhEtyCbl but somewhat shorter, ca. 50 fs, for CNCbl.<sup>43</sup> Stimulated emission is also observed for the PhEtyCbl antivitamin studied earlier following 550 nm excitation.<sup>45</sup>

The absence of significant intensity for wavelengths  $>$ 590 nm in the broadband probe used in most of the measurements of PhEtyCbl prevented the identification of stimulated emission in the prior study,<sup>45</sup> but a stimulated emission contribution is apparent in one data set where the continuum extended to 610 nm (see Figure S2). These data represent clear evidence for fluorescence from the lowest optically allowed  $\pi\pi^*$  excited state of cobalt-containing corrins. A stimulated emission signal is not apparent following ca. 400 nm excitation for any of these molecules (see Figures S2 and S3), suggesting that internal conversion from the higher electronic states does not populate the Franck–Condon region of the state responsible for the  $\alpha\beta$ -band absorption. For longer time delays, the transient absorption signal is independent of excitation wavelength.

Although stimulated emission is clearly observed in the transient absorption measurements, analysis of the shape of the fluorescence spectrum from these data is complicated by the overlapping contributions of ground state bleach, stimulated emission, and excited state absorption. To analyze the spectral shape, we turn to integrated fluorescence measurements. The Strickler–Berg formula<sup>46</sup> can be used to estimate the fluorescence quantum yield. Given an excited state lifetime of 200 fs, an estimated peak extinction coefficient at  $\lambda_{\max} = 550$  nm of ca.  $(8.5 \pm 1.5) \times 10^3 \text{ M}^{-1} \text{ cm}^{-1}$ , a peak fluorescence near 580 nm, and assuming the  $\alpha\beta$  absorption band from 465 to 600 nm is assigned to one electronic transition, the fluorescence quantum yield is estimated to fall between  $5 \times 10^{-6}$  and  $8 \times 10^{-6}$ . The emission lifetime for CNCbl is closer to 50 fs, and the fluorescence quantum yield is estimated to be somewhat lower (ca.  $(1-2) \times 10^{-6}$ ). A separate estimate of the quantum yield can be obtained from recent fluorescence lifetime measurements and quantum yield determinations for the natural cobalt-free corrin Hby<sup>36</sup> and its zinc complex Znby,<sup>35</sup> with fluorescence lifetimes  $\tau_{\text{fl}}$  of 3.3 and  $<$ 0.4 ns,

respectively. If the intrinsic radiative lifetimes of HOPryCbl, F<sub>2</sub>PhEtyCbl, and CNCbl are similar to Hby ( $\tau_r = \tau_{fl}/\phi_{fl} = 3.3 \text{ ns}/0.18 = 18 \text{ ns}$ )<sup>36</sup> and Znby ( $\tau_r = \tau_{fl}/\phi_{fl} = 0.4 \text{ ns}/0.025 = 16 \text{ ns}$ ),<sup>35</sup> the lifetime for stimulated emission of 200 fs in HOPryCbl and F<sub>2</sub>PhEtyCbl corresponds to a slightly higher quantum yield of  $1.2 \times 10^{-5}$ . These yields of  $10^{-6}$ – $10^{-5}$  are small but expected to provide a measurable signal.

The emission spectra of HOPryCbl and CNCbl were probed directly by measuring the time-integrated fluorescence signal as a function of excitation wavelength by using a sensitive steady state fluorometer. The HOPryCbl signal is weak, but varying the excitation wavelength permits separation of Raman scattering, predominantly from the solvent, and cobalamin fluorescence (see Figure S4a). The signal is easily observed and the amplitude scales with sample concentration (see Figure S4c). Emission spectra obtained for three excitation wavelengths at three concentrations are plotted in Figure 4 (see also

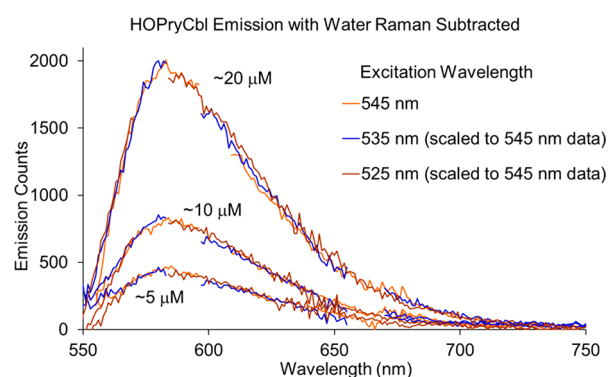


**Figure 4.** HOPryCbl integrated emission for three excitation wavelengths and three solute concentrations. The strong water Raman band has been subtracted out along with the cell background (see Figure S4). This region around 660 nm has been omitted from 535 nm data as subtraction here left a small artifact. The region of the weaker water Raman band near the peak of the fluorescence spectrum has been removed from the data to avoid artifacts in this region. The spectral shape is independent of excitation wavelength and solvent concentration over this range. In particular, the intensity tracks linearly with concentration.

Figures S4 and S5). The CNCbl fluorescence is approximately a factor of 8 weaker than the HOPryCbl fluorescence, making it harder to separate from the strong Raman bands and making it difficult to determine the short wavelength edge of the spectrum accurately (see Figure S6). Fluorescence is also observed for F<sub>2</sub>PhEtyCbl (see Figure S7).

## DISCUSSION

The averaged fluorescence spectra of HOPryCbl and CNCbl are plotted in Figure 5 and compared with the fluorescence spectrum of Znbl reported previously.<sup>35</sup> Analysis of the cobalamin absorption spectrum by us and by others has typically involved fitting the spectrum to a sum of Gaussian bands with the  $\alpha$ ,  $\beta$ , and sh peaks assigned to distinct electronic states or to a vibrational progression in  $\nu_{LA}$ , the long axis C=C stretching mode of the corrin ring, within a single state.<sup>29,40</sup> This mode is observed at ca.  $1500 \text{ cm}^{-1}$  in resonance Raman measurements of cobalt corrins, with the expectation that the frequency is somewhat lower in the excited state, ca.  $1300 \text{ cm}^{-1}$  if the peaks in the absorption spectrum represent a vibrational progression.<sup>29,33</sup> The fluorescence spectrum can

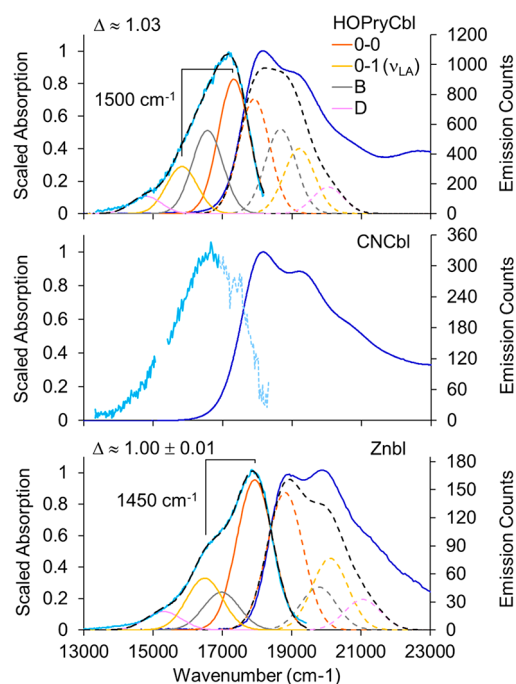


**Figure 5.** Steady state emission spectra of HOPryCbl (top), CNCbl (middle), and Znbl (bottom)<sup>35</sup> compared with the absorption spectra and with a fit of the fluorescence spectra to a sum of four Gaussian bands. The bands designated 0–0 and 0–1 are held at the ground state separation of ca.  $1500 \text{ cm}^{-1}$  for the corrin ring C=C stretching mode  $\nu_{LA}$  implicated in resonance Raman measurements of cobalamins, while the other two bands, B and D, are allowed to vary freely in center wavenumber. See the text and Supporting Information for more details of the fitting. No fit is shown for CNCbl because of uncertainties in the fluorescence peak introduced by reabsorption and by subtraction of the background contribution for these very small signals (see Figure S6).

also be fit to a sum of Gaussians with the constraint that the ground state frequency  $\nu_{LA}$  is fixed to  $1500 \text{ cm}^{-1}$ . The fitting procedure is described in more detail in the Supporting Information. As indicated in Figure 5, the breadth of the emission spectra for all three compounds is consistent with a progression in  $\nu_{LA}$ . The relative intensities of the 0–0 and 0–1 transitions suggest a dimensionless displacement between the ground and excited state of ca.  $\Delta = 1.03$  for HOPryCbl and  $\sim 1.00$  for Znbl. See the Supporting Information for details of the analysis.<sup>29,47–50</sup> These values for the displacement are somewhat lower than 1.28 derived previously for CNCbl and 1.45 obtained for MeCbl<sup>29</sup> but large enough to account for the strong enhancement of this mode in resonance Raman spectra. As illustrated in Figure 5, vibronic structure consistent with a progression in  $\nu_{LA}$  alone is not sufficient to account for the entire emission spectrum. An additional band, B, between the 0–0 and 0–1 transitions is used in the fits to approximate the combined effect of lower frequency vibrational modes. The best fit for this band is at  $\sim 760 \text{ cm}^{-1}$  for HOPryCbl and  $\sim 960 \text{ cm}^{-1}$  for Znbl. A contribution in this frequency range is also identified in the 77 K excitation and emission spectra of Znby (see Figure S8 and discussion in the Supporting Information).

An estimate of the breadth of the absorption spectrum from the ground state to the fluorescent excited state that is consistent with the fit to the fluorescence is also plotted in Figure 5 (see the Supporting Information for details). The measurements reported here demonstrate that the breadth of

the  $\alpha\beta$ -band absorption spectrum of typical cobalamins is dominated by a single electronic transition but must also contain contributions from unique electronic transitions at shorter wavelengths. No attempt is made to fit the absorption spectrum because of the ambiguity introduced by these additional electronic transitions. The visible absorption spectrum is dominated by the  $\pi\pi^*$  transitions of the corrin ring and is similar for typical cobalamins, zinc-substituted analogues,<sup>35</sup> and metal-free Hby.<sup>36</sup> The presence of a Co atom opens a rapid channel for depopulation of the “bright” state. This precipitates the changes in the axial bonding that are observed in time-resolved XANES measurements.<sup>42,43</sup>

## CONCLUSIONS

The measurements reported here demonstrate the presence of short-lived fluorescence from the lowest Franck–Condon active excited state of four typical cobalamins: CNCbl, PhEtyCbl, F<sub>2</sub>PhEtyCbl, and HOPryCbl. This fluorescence disappears as changes in electronic configuration and atomic motions coupled to axial bond elongation move the population out of the bright state into a dark region of the excited state potential energy surface. The breadth of the fluorescence spectrum demonstrates that the visible absorption band is dominated by a single electronic transition, although additional electronic states also contribute. Detailed analysis of the electronic and vibronic structure of cobalamins will require time-resolved measurements of the fluorescence spectrum as a function of excitation wavelength. We have also observed short-lived stimulated emission in transient absorption measurements of AdoCbl, suggesting that this is a common feature of cobalamins excited into the lowest allowed excited state and that rapid motion out of the Franck–Condon region involves changes in the axial bonds.<sup>44</sup> Femtosecond broadband fluorescence measurements will provide additional insight into the factors that differentiate the electronic structure, and thus the structured absorption bands, of “typical” cobalamins such as CNCbl, F<sub>2</sub>PhEtyCbl, and HOPryCbl from the less structured absorption bands of organocobalamins such as the coenzymes MeCbl and AdoCbl.

## ASSOCIATED CONTENT

### Supporting Information

The Supporting Information is available free of charge at <https://pubs.acs.org/doi/10.1021/acs.jpcb.0c04886>.

Additional data figures including transient absorption data figures for PhEtyCbl and for all four compounds following ca. 400 nm excitation, additional fluorescence spectra for HOPryCbl, CNCbl, and F<sub>2</sub>PhEtyCbl, a description of the method used to model the fluorescence and absorption spectra (PDF)

## AUTHOR INFORMATION

### Corresponding Author

**Roseanne J. Sension** – Department of Chemistry and Department of Physics, University of Michigan, Ann Arbor, Michigan 48109-1055, United States; [orcid.org/0000-0001-6758-0132](https://orcid.org/0000-0001-6758-0132); Phone: 734-763-6074; Email: [rsension@umich.edu](mailto:rsension@umich.edu)

### Authors

**Elvin V. Salerno** – Department of Chemistry, University of Michigan, Ann Arbor, Michigan 48109-1055, United States

**Nicholas A. Miller** – Department of Chemistry, University of Michigan, Ann Arbor, Michigan 48109-1055, United States; [orcid.org/0000-0002-9146-5414](https://orcid.org/0000-0002-9146-5414)

**Arkabha Konar** – Department of Physics, University of Michigan, Ann Arbor, Michigan 48109-1040, United States; [orcid.org/0000-0001-6546-4111](https://orcid.org/0000-0001-6546-4111)

**Yan Li** – Department of Chemistry, University of Michigan, Ann Arbor, Michigan 48109-1055, United States

**Christoph Kieninger** – Institute of Organic Chemistry & Center for Molecular Biosciences, University of Innsbruck, A-6020 Innsbruck, Austria

**Bernhard Kräutler** – Institute of Organic Chemistry & Center for Molecular Biosciences, University of Innsbruck, A-6020 Innsbruck, Austria; [orcid.org/0000-0002-2222-0587](https://orcid.org/0000-0002-2222-0587)

Complete contact information is available at:

<https://pubs.acs.org/10.1021/acs.jpcb.0c04886>

## Author Contributions

E.V.S. and N.A.M. contributed equally to this work.

## Notes

The authors declare no competing financial interest.

## ACKNOWLEDGMENTS

We thank Dr. Steffen Jockusch (Columbia University, New York) for the emission spectra of Znbl and Znby. This work was supported by grants from the National Science Foundation NSF-CHE 1464584 and NSF-CHE 1836435 to R.J.S. and NSF-DGE 1256260 to E.V.S. and from the Austrian Science Fund (FWF) project P-28892 to B.K. Portions of this work were performed in the Laboratory for Ultrafast Multidimensional Optical Spectroscopy (LUMOS), supported by NSF-CHE 1428479.

## REFERENCES

- (1) *Photobiology - The Science of Life and Light*, 2nd ed.; Björn, L. O., Ed.; Springer: New York, 2008.
- (2) *Chlorophylls and Bacteriochlorophylls*; Grimm, B., Porra, R., Rüdiger, W., Scheer, H., Eds.; Springer: Dordrecht, 2006; Vol. 25.
- (3) Zimmer, M. GFP: from jellyfish to the Nobel prize and beyond. *Chem. Soc. Rev.* **2009**, *38*, 2823–2832.
- (4) Choi, M. S.; Yamazaki, T.; Yamazaki, I.; Aida, T. Bioinspired molecular design of light-harvesting multiporphyrin arrays. *Angew. Chem., Int. Ed.* **2004**, *43*, 150–158.
- (5) Shell, T. A.; Lawrence, D. S. Vitamin B<sub>12</sub>: A tunable, long wavelength, light-responsive platform for launching therapeutic agents. *Acc. Chem. Res.* **2015**, *48*, 2866–2874.
- (6) Elias-Arnanz, M.; Padmanabhan, S.; Murillo, F. J. Light-dependent gene regulation in nonphototrophic bacteria. *Curr. Opin. Microbiol.* **2011**, *14*, 128–135.
- (7) *Multiporphyrin Arrays - Fundamentals and Applications*; Kim, D., Ed.; Pan Stanford Publishing: Singapore, 2012.
- (8) Rury, A. S.; Wiley, T. E.; Sension, R. J. Energy cascades, excited state dynamics, and photochemistry in cob(III)alamins and ferric porphyrins. *Acc. Chem. Res.* **2015**, *48*, 860–867.
- (9) Toda, M. J.; Lodowski, P.; Al Mamun, A.; Jaworska, M.; Kozłowski, P. M. Photolytic properties of the biologically active forms of vitamin B<sub>12</sub>. *Coord. Chem. Rev.* **2019**, *385*, 20–43.
- (10) Jones, A. R. The photochemistry and photobiology of vitamin B<sub>12</sub>. *Photochem. & Photobiol. Sci.* **2017**, *16*, 820–834.
- (11) Banerjee, R.; Ragsdale, S. W. The many faces of vitamin B<sub>12</sub>: Catalysis by cobalamin-dependent enzymes. *Annu. Rev. Biochem.* **2003**, *72*, 209–247.
- (12) *Chemistry and Biochemistry of B12*; Banerjee, R., Ed.; John Wiley & Sons: New York, 1999.

- (13) Gruber, K.; Puffer, B.; Kräutler, B. Vitamin B<sub>12</sub>-derivatives - enzyme cofactors and ligands of proteins and nucleic acids. *Chem. Soc. Rev.* **2011**, *40*, 4346–4363.
- (14) Drennan, C.; Huang, S.; Drummond, J.; Matthews, R.; Lidwig, M. How a protein binds B<sub>12</sub> - a 3.0-Ångström X-ray structure of B<sub>12</sub>-binding domains of methionine synthase. *Science* **1994**, *266*, 1669–1674.
- (15) Kräutler, B.; Puffer, B. Vitamin B<sub>12</sub>-derivatives: Organometallic catalysts, cofactors and ligands of bio-macromolecules In *Handbook of Porphyrin Science*; Kadish, K. M., Smith, K. M., Guillard, R., Eds.; World Scientific: 2012; Vol. 25, pp 133–265.
- (16) Banerjee, R.; Gherasim, C.; Padovani, D. The tinker, tailor, soldier in intracellular B<sub>12</sub> trafficking. *Curr. Opin. Chem. Biol.* **2009**, *13*, 484–491.
- (17) Padovani, D.; Labunska, T.; Palfey, B. A.; Ballou, D. P.; Banerjee, R. Adenosyltransferase tailors and delivers coenzyme B<sub>12</sub>. *Nat. Chem. Biol.* **2008**, *4*, 194–196.
- (18) Stich, T. A.; Yamanishi, M.; Banerjee, R.; Brunold, T. C. Spectroscopic evidence for the formation of a four-coordinate Co<sup>2+</sup> cobalamin species upon binding to the human ATP: Cobalamin adenosyltransferase. *J. Am. Chem. Soc.* **2005**, *127*, 7660–7661.
- (19) Banerjee, R. Radical carbon skeleton rearrangements: Catalysis by coenzyme B<sub>12</sub>-dependent mutases. *Chem. Rev.* **2003**, *103*, 2083–2094.
- (20) Toraya, T. Radical catalysis in coenzyme B<sub>12</sub>-dependent isomerization (eliminating) reactions. *Chem. Rev.* **2003**, *103*, 2095–2127.
- (21) Matthews, R. G.; Koutmos, M.; Datta, S. Cobalamin-dependent and cobamide-dependent methyltransferases. *Curr. Opin. Struct. Biol.* **2008**, *18*, 658–666.
- (22) Bridwell-Rabb, J.; Drennan, C. L. Vitamin B<sub>12</sub> in the spotlight again. *Curr. Opin. Chem. Biol.* **2017**, *37*, 63–70.
- (23) Ruetz, M.; Salchner, R.; Wurst, K.; Fedosov, S.; Kräutler, B. Phenylethynylcobalamin: A light-stable and thermolysis-resistant organometallic vitamin B<sub>12</sub> derivative prepared by radical synthesis. *Angew. Chem., Int. Ed.* **2013**, *52*, 11406–11409.
- (24) Hisaeda, Y.; Tahara, K.; Shimakoshi, H.; Masuko, T. Bioinspired catalytic reactions with vitamin B<sub>12</sub> derivative and photosensitizers. *Pure Appl. Chem.* **2013**, *85*, 1415–1426.
- (25) Salerno, E. V.; Miller, N. A.; Konar, A.; Salchner, R.; Kieninger, C.; Wurst, K.; Spears, K. G.; Kräutler, B.; Sension, R. J. Exceptional photochemical stability of the Co–C bond of alkynyl cobalamins, potential antivitamin B<sub>12</sub> and core elements of B<sub>12</sub>-based biological vectors. *Inorg. Chem.* **2020**, *59*, 6422–6431.
- (26) Ruetz, M.; Shanmuganathan, A.; Gherasim, C.; Karasik, A.; Salchner, R.; Kieninger, C.; Wurst, K.; Banerjee, R.; Koutmos, M.; Kräutler, B. Antivitamin B<sub>12</sub> inhibition of the human B<sub>12</sub>-processing enzyme CblC: Crystal structure of an inactive ternary complex with glutathione as the cosubstrate. *Angew. Chem., Int. Ed.* **2017**, *56*, 7387–7392.
- (27) Kräutler, B. Antivitamins B<sub>12</sub> - a structure- and reactivity-based concept. *Chem. - Eur. J.* **2015**, *21*, 11280–11287.
- (28) Kozłowski, P. M.; Garabato, B. D.; Lodowski, P.; Jaworska, M. Photolytic properties of cobalamins: A theoretical perspective. *Dalton Trans.* **2016**, *45*, 4457–4470.
- (29) Stich, T. A.; Brooks, A. J.; Buan, N. R.; Brunold, T. C. Spectroscopic and computational studies of Co<sup>3+</sup>-corrinoids: Spectral and electronic properties of the B<sub>12</sub> cofactors and biologically relevant precursors. *J. Am. Chem. Soc.* **2003**, *125*, 5897–5914.
- (30) Ouyang, L.; Randaccio, L.; Rulis, P.; Kurmaev, E. Z.; Moewes, A.; Ching, W. Y. Electronic structure and bonding in vitamin B<sub>12</sub> cyanocobalamin. *J. Mol. Struct.: THEOCHEM* **2003**, *622*, 221–227.
- (31) Lodowski, P.; Jaworska, M.; Kornobis, K.; Andruniow, T.; Kozłowski, P. M. Electronic and structural properties of low-lying excited states of vitamin B<sub>12</sub>. *J. Phys. Chem. B* **2011**, *115*, 13304–13319.
- (32) Andruniow, T.; Kozłowski, P. M.; Zgierski, M. Z. Theoretical analysis of electronic absorption spectra of vitamin B<sub>12</sub> models. *J. Chem. Phys.* **2001**, *115*, 7522–7533.
- (33) Handali, J. D.; Sunden, K. F.; Thompson, B. J.; Neff-Mallon, N. A.; Kaufman, E. M.; Brunold, T. C.; Wright, J. C. Three dimensional triply resonant sum frequency spectroscopy revealing vibronic coupling in cobalamins: Toward a probe of reaction coordinates. *J. Phys. Chem. A* **2018**, *122*, 9031–9042.
- (34) Pratt, J. M. The roles of Co, corrin and protein. II. Electronic spectra and structure of the corrin ligand: Molecular machinery of the protein. In *Chemistry and Biochemistry of B12*; Banerjee, R., Ed.; Wiley: New York, 1999; pp 113–164.
- (35) Kieninger, C.; Baker, J. A.; Podewitz, M.; Wurst, K.; Jockusch, S.; Lawrence, A. D.; Deery, E.; Gruber, K.; Liedl, K. R.; Warren, M. J.; et al. Zinc substitution of cobalt in vitamin B<sub>12</sub>: Zincobyrinic acid and zincobalamin as luminescent structural B<sub>12</sub>-mimics. *Angew. Chem., Int. Ed.* **2019**, *58*, 14568–14572.
- (36) Kieninger, C.; Deery, E.; Lawrence, A. D.; Podewitz, M.; Wurst, K.; Nemoto-Smith, E.; Widner, F. J.; Baker, J. A.; Jockusch, S.; Kreutz, C. R.; Liedl, K. R.; Gruber, K.; Warren, M. J.; Kräutler, B. The hydrogenobyrinic acid structure reveals the corrin ligand as an entatic state module empowering B<sub>12</sub>-cofactors for catalysis. *Angew. Chem., Int. Ed.* **2019**, *58*, 10756–10760.
- (37) Fugate, R. D.; Chin, C.-A.; Song, P.-S. A spectroscopic analysis of vitamin B<sub>12</sub> derivatives. *Biochim. Biophys. Acta, Gen. Subj.* **1976**, *421*, 1–11.
- (38) Thomson, A. J. Polarized fluorescence spectra of some naturally occurring corrins. *J. Am. Chem. Soc.* **1969**, *91*, 2780–2785.
- (39) Gardiner, M.; Thomson, A. J. Luminescence properties of some synthetic metalcorrins. *J. Chem. Soc., Dalton Trans.* **1974**, 820–828.
- (40) Wiley, T. E.; Miller, N. A.; Miller, W. R.; Sofferman, D. L.; Lodowski, P.; Toda, M. J.; Jaworska, M.; Kozłowski, P. M.; Sension, R. J. Off to the races: Comparison of excited state dynamics in vitamin B<sub>12</sub> derivatives hydroxocobalamin and aquocobalamin. *J. Phys. Chem. A* **2018**, *122*, 6693–6703.
- (41) Wiley, T. E.; Arruda, B. C.; Miller, N. A.; Lenard, M.; Sension, R. J. Excited electronic states and internal conversion in cyanocobalamin. *Chin. Chem. Lett.* **2015**, *26*, 439–443.
- (42) Miller, N. A.; Deb, A.; Alonso-Mori, R.; Glownia, J. M.; Kiefer, L. M.; Konar, A.; Michocki, L. B.; Sikorski, M.; Sofferman, D. L.; Song, S.; et al. Ultrafast X-ray absorption near edge structure reveals ballistic excited state structural dynamics. *J. Phys. Chem. A* **2018**, *122*, 4963–4971.
- (43) Miller, N. A.; Deb, A.; Alonso-Mori, R.; Garabato, B. D.; Glownia, J. M.; Kiefer, L. M.; Koralek, J.; Sikorski, M.; Spears, K. G.; Wiley, T. E.; et al. Polarized XANES monitors femtosecond structural evolution of photoexcited vitamin B<sub>12</sub>. *J. Am. Chem. Soc.* **2017**, *139*, 1894–1899.
- (44) Miller, N. A.; Michocki, L. B.; Konar, A.; Alonso-Mori, R.; Deb, A.; Glownia, J. M.; Sofferman, D. L.; Song, S.; Kozłowski, P. M.; Kubarych, K. J.; et al. Ultrafast XANES monitors sequential structural evolution in photoexcited coenzyme B<sub>12</sub>. *J. Phys. Chem. B* **2020**, *124*, 199–209.
- (45) Miller, N. A.; Wiley, T. E.; Spears, K. G.; Ruetz, M.; Kieninger, C.; Kräutler, B.; Sension, R. J. Toward the design of photoresponsive conditional antivitamin B<sub>12</sub>: A transient absorption study of an arylcobalamin and an alkynylcobalamin. *J. Am. Chem. Soc.* **2016**, *138*, 14250–14256.
- (46) Strickler, S. J.; Berg, R. A. Relationship between absorption intensity and fluorescence lifetime of molecule. *J. Chem. Phys.* **1962**, *37*, 814–822.
- (47) McHale, J. L. *Molecular Spectroscopy*, 2nd ed.; CRC Press: Boca Raton, FL, 2017.
- (48) Kelley, A. M. *Condensed-Phase Molecular Spectroscopy and Photophysics*; John Wiley & Sons, Inc.: Hoboken, NJ, 2013.
- (49) Sension, R. J.; Strauss, H. L. Comparison of experiment and theory for the resonance Raman-spectrum of I<sub>2</sub> in solution. I. The Raman excitation profile of I<sub>2</sub> in normal-hexane. *J. Chem. Phys.* **1986**, *85*, 3791–3806.
- (50) Manneback, C. Computation of the intensities of vibrational spectra of electronic bands in diatomic molecules. *Physica* **1951**, *17*, 1001–1010.